Available online at www.sciencedirect.com
SCIENCE DIRECT®
Journal of Photochemistry and Photobiology A: Chemistry 162 (2004) 9–16
Journal of Photochemistry and Photobiology A:Chemistry
www.elsevier.com/locate/jphotochem

# Photosensitization with anthraquinone derivatives: optical and EPR spin trapping studies of photogeneration of reactive oxygen species

K.K. Mothilal [a], J. Johnson Inbaraj [b,1], R. Gandhidasan [b], R. Murugesan [b,*]

[a] *Department of Chemistry, Saraswathi Narayanan College, Madurai 625 022, India*
[b] *School of Chemistry, Madurai Kamaraj University, Madurai 625 021, India*

Received 6 January 2003; received in revised form 12 May 2003; accepted 4 June 2003

**Abstract**

Photodynamic properties of three synthetic anthraquinone derivatives are studied. Efficiency of singlet oxygen generation (by *N*,*N*-dimethyl-4-nitrosoaniline bleaching assay and electron paramagnetic resonance (EPR)-2,2,6,6-tetramethyl-4-piperidinol assay) and rate of superoxide generation (by superoxide dismutase inhibitable ferricytochrome *c* reduction assay and EPR spin trapping assay) of 2-(1-hydroxyethyl)quinizarin (HQ), 2-acetylquinizarin (AQ) and quinizarin (QZ) are determined. The singlet oxygen generating efficiency follows the order: HQ > AQ > QZ. Irradiation in the presence of specific $^1O_2$ quenchers such as 1,4-diazabicyclo[2,2,2]-octane and sodium azide lends supportive evidence for the formation of $^1O_2$. Photolysis of HQ in dimethyl sulphoxide in the presence of 5,5-dimethyl-1-pyrroline-*N*-oxide generates a multiline EPR spectrum characteristic of mixture of spin adducts corresponding to superoxide anion and hydroxyl radical. Electron donors such as reduced nicotinamide adenine dinucleotide (NADH), ethylenediaminetetra acetic acid and diethyltriaminopenta acetic acid are found to enhance the yield of $O_2^{\bullet -}$ EPR study further reveals that in aqueous solution, the superoxide radical anion formed rapidly transforms to hydroxyl radical. Enzymatic reduction of HQ, AQ and QZ in dark by incubation with NADH-cytochrome *c* reductase generates $O_2^{\bullet -}$ and the efficiency follows the order: HQ > AQ > QZ. Cyclic voltammetric studies indicate a correlation between this order and the redox potential of the quinones.


*Keywords:* ROS; Spin trapping; DMPO; Anthraquinone; Superoxide; Generation

## 1. Introduction

Large number of anthraquinones, both synthetic and naturally occurring, have been screened for their antitumour activity in a variety of animal test systems [1–3]. Anthracycline derivatives constitute an important class of anticancer drugs [4,5]. Many such anthraquinone derivatives possess the ability to mediate one electron transfer to molecular oxygen to form superoxide anion radical and to generate reactive oxygen species (ROS) upon visible light illumination. Ketoreduction, clevage reactions and conjugation are the three important types of anthracycline metabolic reactions. During the anthracycline cleavage to aglycone, an anthracycline radical is formed, in the presence of molecular oxygen, undergoes redox cycling to form ROS [6]. Anthracycline derivatives such as damnacanthal and nordamnacanthal possess biological properties which are strongly light dependent reactions [7]. Photoinduced production of superoxide anion radicals by adriamycin and daunorubicin is well known [8]. Some aminoanthraquinones have also been studied for their efficiency to generate ROS upon visible light illumination [9,10]. Since there is considerable interest in the photodynamic activity of anthraquinones, we have earlier investigated photodynamic action as well as enzymatic reduction of some naturally occurring anthraquinones. Due to the current interest in understanding the factors contributing to the photodynamic activity of anthraquinones [11–13], the present study reports the photogeneration of ROS from three synthetic anthraquinones. These three anthraquinones possess hydroxyl groups in 1,4 positions, but differ in the substituents at position 2. Hence the present study was attempted to understand the substituents effects

*Abbreviations:* RNO, *N*,*N*-dimethyl-4-nitrosoaniline; ROS, reactive oxygen species; TEMPL, 2,2,6,6-tetramethyl-4-piperidinol; TEMPOL, 2,2,6,6-tetramethyl-4-piperidinol-*N*-oxyl; SOD, superoxide dismutase; DMPO, 5,5-dimethyl-1-pyrroline-*N*-oxide; DABCO, 1,4-diazabicyclo [2,2,2]-octane; RB, rose bengal; EDTA, ethylenediaminetetra acetic acid; NADH, reduced nicotinamide adenine dinucleotide; DETAPAC, diethyltriaminopenta acetic acid; EPR, electron paramagnetic resonance; DMSO, dimethyl sulphoxide

* Corresponding author. Fax: +91-452-2459105.
*E-mail address:* rammurugesan@yahoo.com (R. Murugesan).
[1] Present address: Laboratory of Pharmacology and Chemistry, National Institute of Environmental Health Sciences, National Institutes of Health, Research Triangle Park, NC, USA.

1010-6030/$ – see front matter © 2004 Elsevier B.V. All rights reserved.
doi:10.1016/S1010-6030(03)00290-9

on the generation of ROS. Also we have studied the effect of electron donors such as reduced nicotinamide adenine dinucleotide (NADH), ethylenediaminetetra acetic acid (EDTA) and diethyltriaminopenta acetic acid (DETAPAC) on the efficiencies of generation of $O_2^{\bullet -}$ by these anthraquinones.

## 2. Experimental section

### 2.1. Chemicals

1,4-Dihydroxyanthraquinone (quinizarin, QZ) was purchased from Aldrich and used without additional purification. *N*,*N*-Dimethyl-4-nitrosoaniline (RNO), 5,5-dimethyl-1-pyrroline-*N*-oxide (DMPO), 1,4-diazabicyclo[2,2,2]-octane (DABCO), DETAPAC and rose bengal (RB) were obtained from Aldrich. Imidazole, EDTA and sodium azide were purchased from S.D.Fine Chemicals. 2,2,6,6-Tetramethyl-4-piperidinol (TEMPL) was obtained from Merck. Superoxide dismutase (SOD), cytochrome *c* reductase and catalase were purchased from Sigma while NADH was obtained from Boehringer Mannheim. Dimethyl sulphoxide (DMSO) (HPLC grade) from Qualigens fine chemicals was used as such. Doubly distilled water was used for all the experiments. Imidazole was used after repeated crystallization from doubly distilled water. All other compounds were used as received. The concentration of the spin trap DMPO was determined spectrophotometrically using $\varepsilon_{227} = 8000\,M^{-1}\,cm^{-1}$.

### 2.2. Preparation of anthraquinone derivatives

2-Acetylquinizarin (AQ) and 2-(1-hydroxyethyl)quinizarin (HQ) were prepared by following the reported procedure [12].

#### 2.2.1. Preparation of leuco-quinizarin

To a solution of QZ (2.19 g) in methylene chloride (170 ml) zinc powder (6 g) was added. The mixture was degassed for 5 min and placed under nitrogen. Glacial acetic acid (13 ml) was added via a septum over a period of 5 min and the mixture was stirred at room temperature for 6 h. Zinc was removed by filtration through a plug of celite and the filtrate was washed with water (3× 175 ml). After drying over magnesium sulphate and filtering, the solvent was removed under reduced pressure and the dark yellow residue was crystallized from *n*-hexane to yield yellow plates of leuco-quinizarin.

#### 2.2.2. Preparation of HQ

A two necked flask was charged with leuco-quinizarin (945 mg) and fitted with a septum and a pressure-equalizing funnel containing a solution of potassium hydroxide (2.3 g) in methanol (80 ml). The mixture was degassed for 5 min and placed under nitrogen. A solution of methanolic potassium hydroxide (0.01 M) was added with stirring. The resulting deep yellow solution was cooled to 0 °C and acetaldehyde (0.85 ml) was added using a syringe over a period of 5 min and then stirred for 7 h. It was then aerated for 10 min. On acidification with concentrated hydrochloric acid an orange precipitate was formed which was extracted with methylene chloride (4× 50 ml), dried over magnesium sulphate, filtered and evaporated. The product was purified by silica gel column chromatography, eluting with methylene chloride and ethyl acetate mixture.

#### 2.2.3. Preparation of AQ

To a stirred solution of the HQ (376 mg) in acetone (60 ml) was added celite (3 g). Jones reagent was added dropwise until the starting material was shown to be absent by TLC. After filtration, the solution was poured into cold water (50 ml) and extracted with methylene chloride (4× 20 ml). The organic phase was dried over magnesium sulphate, filtered and evaporated to give AQ.

These two compounds (HQ and AQ) were characterized by $^1$HNMR spectra on a JEOL GSX 400 spectrometer with tetramethylsilane as internal standard. NMR spectral data (Chemical shift in $\delta$, ppm) for HQ: 13.25 (1H, s, OH-1), 1.55 (3H, d, $CH_3$-2), 2.35 (1H, bs, OH-2), 5.25 (1H, q, CH-2), 7.50 (1H, s, H-3), 12.65 (1H, s, OH-4), 8.40 (2H, m, H-5′,8′), 7.90 (2H, m, H-6′,7′). NMR spectral data for AQ: 13.8 (1H, s, OH-1), 2.77 (3H, s, $COCH_3$), 7.73 (1H, s, H-3), 12.6 (1H, s, OH-4), 8.4 (2H, m, H-5′,8′), 7.90 (2H, m, H-6′,7′). The chemical structures of these quinones are given in Fig. 1 along with their absorption maxima.

### 2.3. Cyclic voltammetry

The cyclic voltammetry (CV) experiments were performed with electrochemical analyser BAS 50. A three electrode assembly of glassy carbon electrode (working), platinum electrode (auxiliary) and Ag/AgCl (reference)

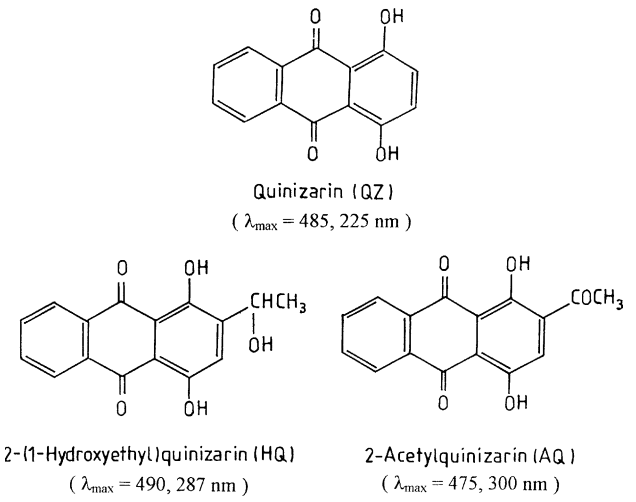


Fig. 1. Chemical structures of QZ, AQ and HQ with their absorption maxima.

was used. Glassy carbon electrode was resurfaced with alumina. Solutions of quinones (1 mg, 5 ml of acetonitrile) were prepared in HPLC grade acetonitrile containing 0.05 M tetrabutylammonium perchlorate (TBAP) as supporting electrolyte. Each solution was purged with nitrogen for 10 min prior to measurement and the cyclic voltammograms were recorded under nitrogen atmosphere. The redox potentials given are against Ag/AgCl, unless otherwise mentioned.

### 2.4. Light source

A 150 W xenon lamp was used for photolysis. A filter combination of 10 cm of potassium iodide solution (1 g in 100 ml of water) plus 1 cm of pyridine was used to cut-off below 300 nm and to get a spectral window 300–700 nm. The reaction mixture in a quartz cuvette placed at a distance of 12 cm from the light source was continuously stirred during irradiation. The irradiation was generally carried out in an open cuvette in equilibrium with atmosphere.

### 2.5. Optical assay

#### 2.5.1. Singlet oxygen detection

The detection of singlet oxygen was performed by RNO bleaching assay [13]. The detailed experimental procedure is as given in our earlier publication [14].

#### 2.5.2. Superoxide detection

The formation of superoxide was estimated by SOD inhibitable cytochrome *c* reduction method [15]. Solution of anthraquinones (100 μM) were photolysed in the presence of ferricytochrome *c* (50 μM) in 50 mM phosphate buffer (pH = 7.4). The reduction was monitored spectrophotometrically at 550 nm, where $\varepsilon_{max}$ for ferricytochrome *c* is $0.99 \times 10^4\ M^{-1}\ cm^{-1}$ and $\varepsilon_{max}$ for ferrocytochrome *c* is $2.99 \times 10^4\ M^{-1}\ cm^{-1}$. Hence $\Delta\varepsilon_{550} = 20\,000\ M^{-1}\ cm^{-1}$ was used for reduced–oxidized cytochrome *c* [16,17].

To study enzymatic production of superoxide, the reduction of ferricytochrome *c* (50 μM) in the presence of NADH (3 mM), cytochrome *c* reductase (30 mg/ml) and sensitizers (200 μM) in 50 mM phosphate buffer solution (pH = 7.4) was monitored spectrophotometrically at 550 nm [18].

### 2.6. Electron paramagnetic resonance (EPR) measurements

A JEOL JES-TE100 ESR spectrometer was used for EPR measurements. The following parameters were set for the measurements: microwave power, 10 mW; modulation amplitude, 0.01 mT; modulation frequency, 100 kHz.

#### 2.6.1. Detection of singlet oxygen

The photogeneration of $^1O_2$ by anthraquinones can be readily studied by EPR spectroscopy [19]. Reaction mixture (1 ml) containing 10 mM TEMPL and anthraquinones (100 μM) in DMSO was irradiated and the increase in EPR signal intensity with irradiation time was followed. Reaction mixture (150 μM) was drawn into gas permeable Teflon capillary tube (0.8 mm side diameter, 0.5 mm wall thickness) which was folded and inserted into a narrow quartz tube and placed in the EPR cavity for measurements.

#### 2.6.2. Detection of superoxide anion

Spin trapping experiments were used to determine the production of superoxide anion on irradiation of sensitizers. Solutions of anthraquinones (100 μM) were irradiated in the presence of 50 mM DMPO in DMSO. Experiments were repeated to monitor the signal intensity at different intervals of irradiation time. A BASIC program was used to simulate the EPR spectra.

## 3. Results and discussion

### 3.1. Singlet oxygen generation

#### 3.1.1. RNO bleaching assay

Fig. 2 shows the decrease in RNO absorbance at 440 nm of 100 μM of QZ, HQ, AQ and RB as a function of irradiation time. The bleaching of RNO is caused by the transannular peroxide intermediate formed as a result of reaction between photogenerated $^1O_2$ and imidazole. SOD (40 μg/ml) and catalase (40 μg/ml), which remove $O_2^{\bullet -}$ and $H_2O_2$ from the reaction mixture respectively were added to permit the detection and quantification of $^1O_2$ production, without interference from OH radical. The rate of disappearance of quencher (*A*) obeys the following equation [20]:

$$\frac{d[A]}{dt} = I_{ab}\Phi^1O_2\frac{k_r[A]}{k_d}$$

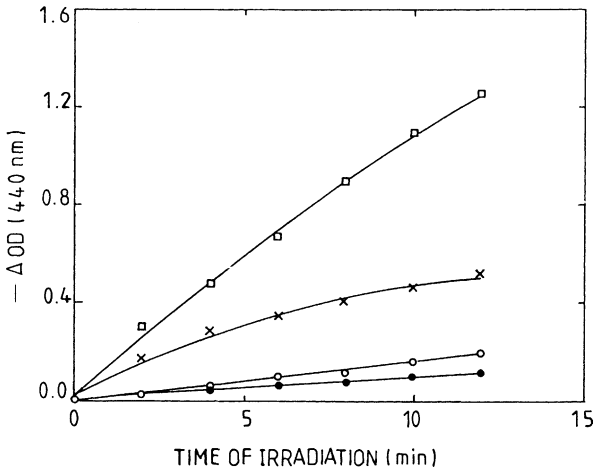


Fig. 2. Photosensitized RNO (50 μM) bleaching measured at 440 nm in the presence of imidazole (10 mM) in 50 mM phosphate buffer (pH = 7.4) with RB (□), QZ (●), HQ (×) and AQ (○) as a function of illumination of time in minutes. The slope was calculated by fitting the experimental data to a second order polynomial.

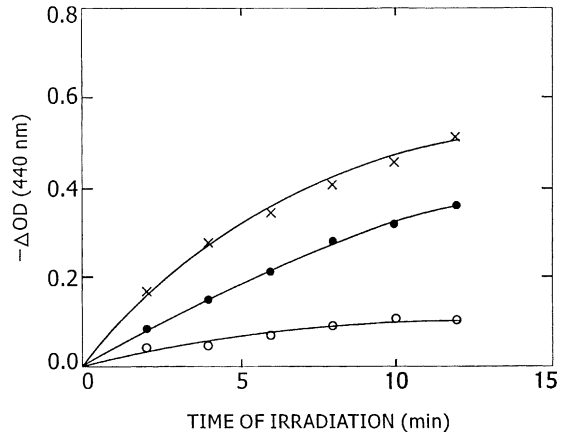


Fig. 3. Inhibition of photosensitized RNO bleaching by HQ in the absence (×) and in the presence of 10 mM DABCO (●) and 0.1 mM sodium azide (○). [Imidazole] = 10 mM.

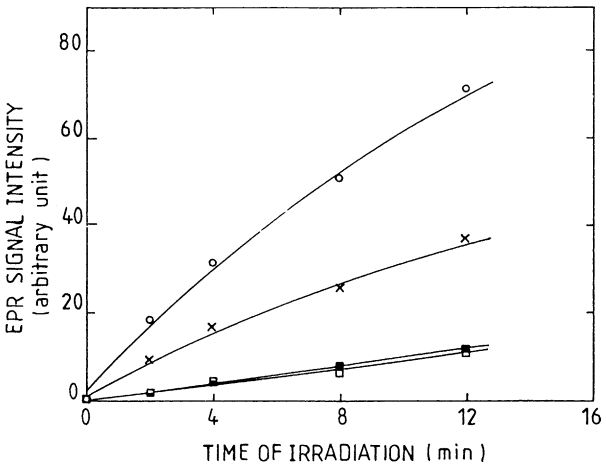


Fig. 4. Production of TEMPOL as a function of irradiation time for different sensitizers (100 μM), RB (○), QZ (□), HQ (×) and AQ (■) in the presence of TEMPL (10 mM) at room temperature in DMSO. Spectrometer settings—microwave power: 2 mW; modulation frequency: 100 kHz; modulation amplitude: 0.1 mT; gain level: $6.3 \times 10^3$; time constant: 0.1 s; scan rate: 4 min.

where $k_r$ is the rate constant for chemical quenching, $k_d$ the rate constant for deactivation of $^1O_2$ by the solvent and $I_{ab}$ the intensity of light absorbed by the sensitizer. The slope of the first order plot is $I_{ab}\ \Phi^1O_2\ (k_r/k_d)$. The slope was calculated by curve fitting the experimental data. The slopes were corrected for molar absorption and photon energy. The singlet oxygen generating efficiencies of the sensitizers were evaluated taking $\Phi^1O_2$ of RB as 0.76 [13,14]. The relative singlet oxygen yields thus evaluated are 0.40, 0.098 and 0.092 for HQ, AQ and QZ, respectively.

Studying the effect of two inhibitors of $^1O_2$ (DABCO and sodium azide) provided further support for the production of singlet oxygen during photosensitization. Inhibition of RNO bleaching by these inhibitors is typically shown for HQ in Fig. 3. The singlet oxygen quenching rate constants of imidazole ($2 \times 10^7\ M^{-1}\ s^{-1}$) and DABCO ($1.5 \times 10^7\ M^{-1}\ s^{-1}$) are comparable [21]. Since the quenching rate constants of equimolar amounts (10 mM) of imidazole and DABCO are similar, both of these compounds would decrease the observed rate by about half, when compared to the rate of RNO bleaching in the absence of DABCO [21]. In the present study, the measurements are carried out in the presence of imidazole (10 mM) and DABCO (10 mM), so the rate of RNO bleaching is decreased to about 25% (0.12), when compared to the rate RNO bleaching in the absence of DABCO. Similarly, sodium azide reacts with $^1O_2$ about 100 times faster than imidazole. The concentration of sodium azide and imidazole used are 0.1 and 10 mM, respectively. Hence at these concentrations, it was found that the RNO bleaching was inhibited by about 50% (0.058). These results confirm the generation of singlet oxygen during the photosensitization process. Similar inhibition of RNO bleaching was also observed when AQ and QZ were photolysed in the presence of DABCO and azide.

### 3.1.2. Electron paramagnetic resonance spectroscopy

Photogeneration of ROS may be due to either Type I or Type II reaction. The Type I reaction involves electron transfer from the sensitizer leading to the formation of superoxide anion. Type II reaction involves transfer of excitation energy from the triplet excited photosensitizer to ground state triplet oxygen, forming singlet oxygen. Numerous photosensitized reactions of quinones of biological important molecules have been ascribed to Type II processes. The production of singlet oxygen during photosensitization of quinones was also studied by EPR spectroscopy. An EPR spectrum consisting of three equally intense lines, characteristic of nitroxide radical (2,2,6,6-tetramethyl-4-piperidinol-*N*-oxyl, TEMPOL) was observed when an aerated solution of quinone and TEMPL was illuminated at room temperature. The formation of TEMPOL from TEMPL is due to the oxidation by $^1O_2$ as shown below (Eq. (1))

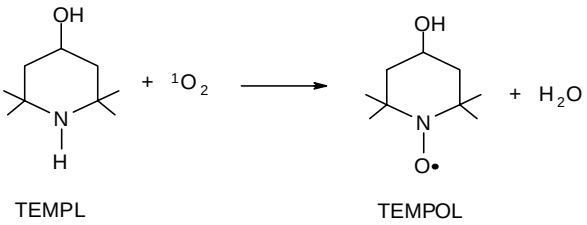


(1)

The hyperfine coupling constant observed (1.55 mT) was identical with that of an authentic sample of TEMPOL. The intensity of the EPR signal was found to increase with increase of irradiation time as shown in Fig. 4. Under similar conditions, irradiation of TEMPL with RB also showed the formation of the three-line EPR spectrum. The singlet oxygen generating efficiency ratio of RB, HQ, AQ and QZ was found to be 1:0.56:0.15:0.11, respectively are comparable to the values obtained by the RNO bleaching assay. During the exposure of solutions without quinones, no EPR signal was obtained even for prolonged irradiation. Similarly the EPR signal was also not observed in dark. These results

suggest that anthraquinones generate singlet oxygen based on Type II mechanism.

### 3.2. Superoxide generation

#### 3.2.1. SOD inhibitable cytochrome c reduction assay

In aqueous medium, the generation of superoxide from the sensitizer could be readily studied by using ferricytochrome *c* reduction assay according to the Eq. (2) [14]

$$\text{Cyt}\,c\,(\text{Fe(III)}) + O_2^{\bullet -} \rightarrow O_2 + \text{Cyt}\,c\,(\text{Fe(II)}) \quad (2)$$

Fig. 5 shows the reduction of cytochrome *c* as a function of irradiation time when air saturated solutions of the sensitizers were photolysed in the presence of 50 μM cytochrome *c* in phosphate buffer (50 mM and pH = 7.4). The rate of superoxide generation was arrived to be 0.115, 0.045 and 0.02 μM/s for HQ, AQ and QZ, respectively. Addition of SOD (50 μg/ml) was found to inhibit the cytochrome *c* reduction. Control experiments indicated that sensitizer, oxygen and light were all essential for the reduction of ferricytochrome *c*.

Fig. 6 shows the effect of electron donor such as EDTA on the rate of cytochrome *c* reduction. EDTA showed a nearly 2–3-fold enhancement in superoxide production. The rates of reduction were found to be 0.24, 0.11 and 0.035 μM/s for HQ, AQ and QZ, respectively in the presence of [10 mM] EDTA, compared to the values of 0.115, 0.045 and 0.002 in the absence of EDTA. Another electron donor, DETAPAC was also found to enhance the superoxide production from HQ although to a lesser extent than EDTA [17]. However the electron donor NADH (0.1 mM) enhanced the superoxide yields by a factor of 25, 18 and 15 in the case of HQ, AQ and QZ, respectively (data not shown). The electron donors (NADH, EDTA and DETAPAC) may interact effectively with the excited state of quinones leading to the generation of $Q^-$ species. Depending on the condition $Q^-$ can then interact with molecular oxygen to yield superoxide anion as shown in Scheme 1.

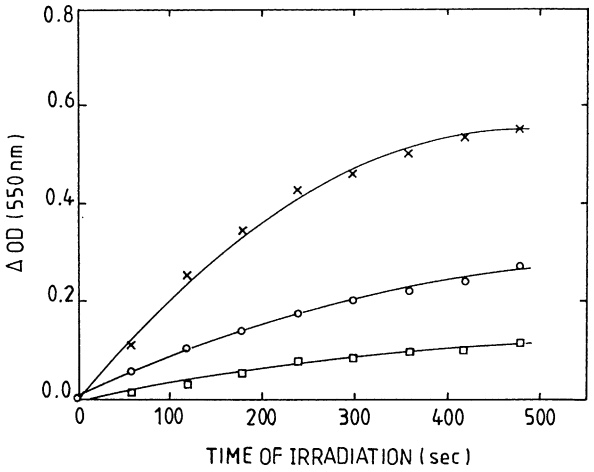


Fig. 5. Photosensitized superoxide generation measured as the rate of cytochrome *c* reduction in the presence of ferricytochrome *c* (50 μM) in 50 mM phosphate buffer pH 7.4 with HQ (×), AQ (○) and QZ (□).

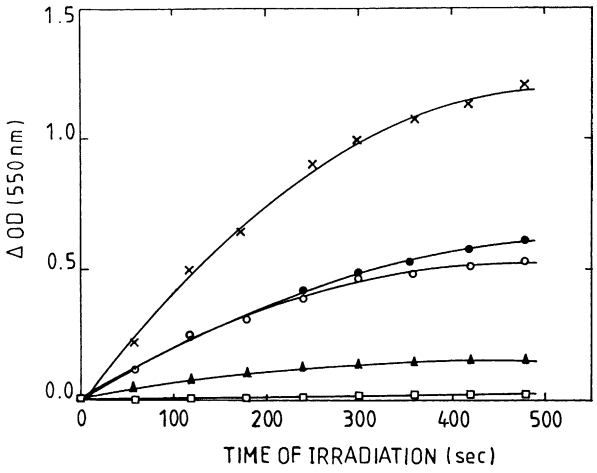


Fig. 6. Photosensitized cytochrome *c* reduction in 50 mM phosphate buffer (pH 7.4) in the presence of EDTA by HQ (×), AQ (○), QZ (▲) and HQ + SOD (40 μg/ml) (□), and in the presence of DETAPAC by HQ (●) as a function of irradiation time.

#### 3.2.2. EPR spin trapping assay

Production of $O_2^{\bullet -}$ from these sensitizers on photoillumination was also studied by EPR spin trapping experiments using DMPO as the spin trap. EPR spin trapping studies were carried out in DMSO because of the longer life time of DMPO-$O_2^{\bullet -}$ in DMSO [22–24]. No EPR signal was observed when DMPO alone was irradiated in DMSO or when the experiment was performed in dark (Fig. 7a). Fig. 7b shows the multiline EPR spectrum obtained when HQ solution containing DMPO was illuminated in air saturated DMSO. The spectrum can readily be analysed in terms of a mixture of two types of DMPO adducts. Adduct I was assigned to DMPO-$O_2^{\bullet -}$, based on its hfc $a_N = 1.3$ mT, $a_H^\beta = 1.054$ mT and $a_H^\gamma = 0.14$ mT. Adduct II was identified as DMPO-OH, with hfc $a_N = 1.4$ mT and $a_H^\beta = 1.163$ mT. The EPR spectra of these two adduct were computer simulated separately using the above hfc values. When these two spectra were combined in the ratio of 85:15 for $O_2^{\bullet -}$ and –OH, respectively, the computer simulated spectrum (Fig. 7c) matched well with the experimentally observed

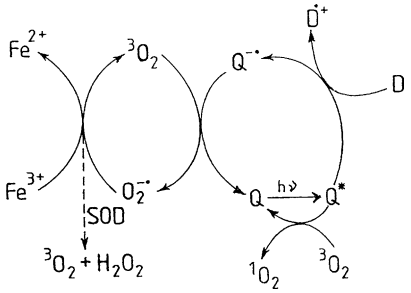


Scheme 1.

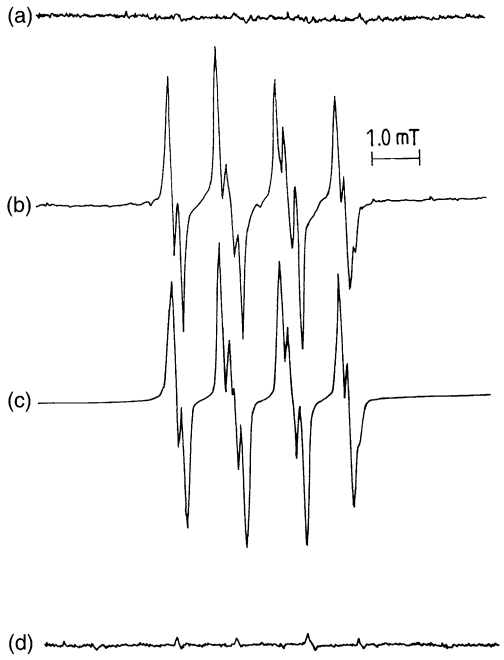


Fig. 7. EPR spectrum obtained by photolysis of HQ (100 μM) in air saturated DMSO solution containing DMPO (50 mM). (a) In the dark; (b) after 4 min irradiation; (c) computer simulated spectrum obtained by the combination of two spin adducts. The spectrum contains two spin adducts: DMPO-$O_2^{\bullet-}$ ($a_N = 1.3$ mT, $a_H^\beta = 1.054$ mT and $a_H^\gamma = 0.14$ mT) and DMPO-OH ($a_N = 1.4$ mT and $a_H^\beta = 1.163$ mT) in the ratio of 85:15. (d) After 4 min irradiation in the presence of SOD (40 μg/ml). Spectrometer settings—microwave power: 10 mW; modulation amplitude: 0.1 mT; gain level: $6.3 \times 10^3$; time constant: 0.1 s; scan rate: 4 min.

one. Addition of SOD (40 μg/ml) prior to illumination inhibited the generation of spin adducts as shown in Fig. 7d. These observations reveal the formation of DMPO-$O_2^{\bullet-}$ as the primary product, which may later decompose to yield the observed DMPO-OH adduct as given in Eq. (3)

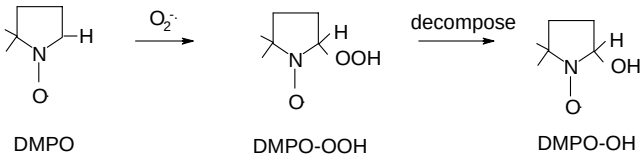


(3)

AQ and QZ also gave the DMPO-$O_2^{\bullet-}$ adduct when they were photolysed in the presence of DMPO in air saturated DMSO solution. The EPR signal intensity, DMPO-$O_2^{\bullet-}$ adduct of all the three anthraquinones were found to increase with irradiation time (Fig. 8). When HQ was irradiated in the presence of DETAPAC (0.01 M) and DMPO (50 mM) in air saturated phosphate buffer (50 mM, pH = 7.4), a four line EPR spectrum ($a_N = a_H^\beta = 1.49$ mT) with an intensity ratio of 1:2:2:1 was observed (Fig. 9). This spectrum corresponds to the hydroxyl radical spin adduct of DMPO [25]. The EPR signal intensity of DMPO-OH adduct was found to increase with increase of irradiation time (Fig. 9b–d). No EPR signals

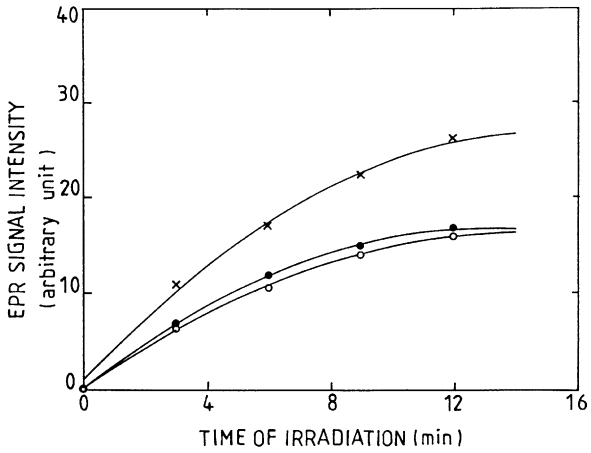


Fig. 8. The EPR signal intensity of DMPO-$O_2^{\bullet-}$ adduct in air saturated DMSO solution containing HQ (×), AQ (●) and QZ (○) as a function of irradiation time.

of DMPO-OH adduct was detected when the $N_2$ saturated solution of HQ was photolysed. Control experiments ensured that no signal was obtained without light, oxygen, HQ and DMPO (Fig. 9a). The formation of DMPO-OH adduct may be due to the decomposition of the unstable DMPO-$O_2^{\bullet-}$ adduct in the protic solvent [23,26–29].

### 3.3. Enzymatic production of superoxide

To study the generation of superoxide from anthraquinones in dark, reduction of cytochrome *c* by the quinones

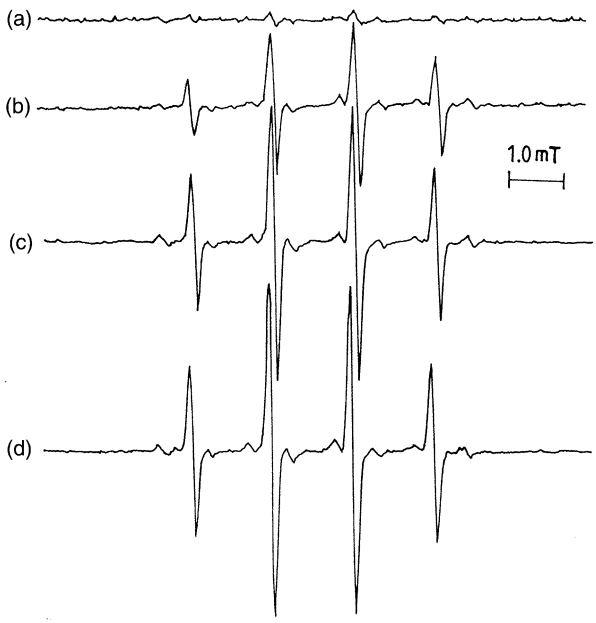


Fig. 9. EPR spectrum observed from HQ (100 μM) and DMPO in phosphate buffer (50 mM, pH = 7.4) before (a) and after irradiation for (b) 3 min, (c) 6 min and (d) 9 min. Spectrometer settings—microwave power: 10 mW; modulation amplitude: 0.1 mT; gain level: $6.3 \times 10^3$; time constant: 0.25 s; scan rate: 4 min.

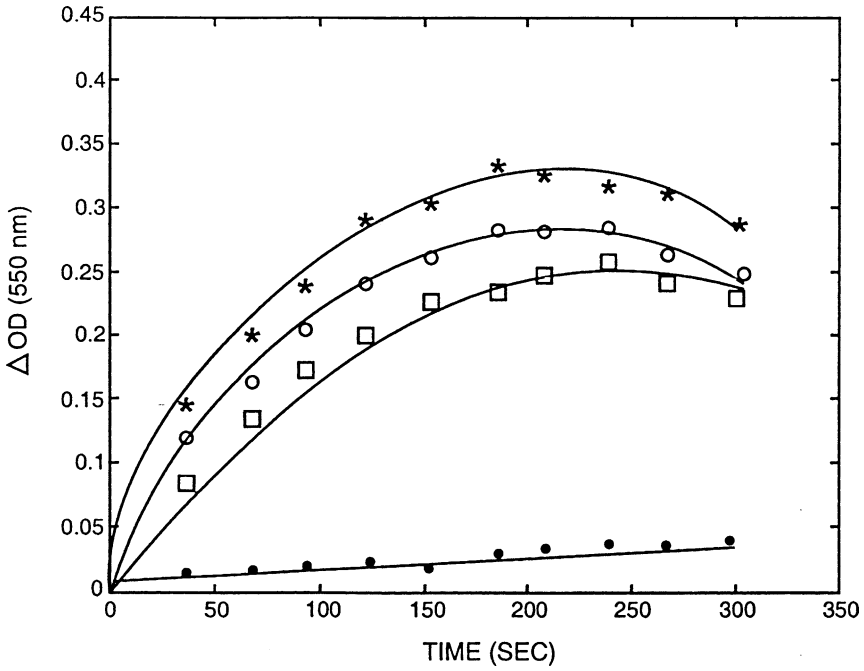


Fig. 10. Enzymatic reduction of cytochrome *c* in the presence of quinones (200 μM) in 50 mM phosphate buffer (pH = 7.4) and in the presence of NADH and cytochrome *c* reductase. Control: Cyt *c* + NADH + Cyt *c* reductase (●); control + HQ (✱); control + AQ (○); control + QZ (□).

in the presence of cytochrome reductase was evaluated. Fig. 10 shows the reduction of cytochrome *c* in dark when air saturated solution of NADH (3 mM), cytochrome *c* reductase (30 mg/ml) in 50 mM phosphate buffer solution was incubated with the quinones (200 μM). The reduction rate of HQ, AQ and QZ on cytochrome *c* in dark are 0.0028, 0.0020 and 0.0021 μM/s, respectively. Addition of SOD inhibited the rate of cytochrome *c* reduction [24] confirming the enzymatic generation of $O_2^{\bullet -}$.

### 3.4. Redox cycling

CV has been extensively used to study the mechanism of anthraquinone mediated superoxide generation [8,30–32]. Drugs like adriamycin and daunorubicin are extensively studied by electrochemical methods [33,34] and there is clear evidence that redox reaction and covalent binding to DNA are necessary for their cytotoxicity. There is an approximate linear correlation between the rate of reduction and reduction potential when simple nitrobenzene, quinones are reduced by cytochrome P450 reductase [35]. To correlate enzymatic generation of $O_2^{\bullet -}$ with the redox potential of the sensitizers (HQ, AQ and QZ), cyclic voltammograms of all the three anthraquinones were measured in the range of +0.5 to −1.5 V. All sensitizers gave well-defined waves of two cathodic and two anodic processes. The cathodic, anodic peak potentials and the $\Delta E_p$ ($E_{pc} - E_{pa}$) values obtained from cyclic voltammograms are collected in Table 1. The cathodic peak at more negative reduction potential may be assigned to the one electron reduction of oxygen (dissolved in DMSO) to the superoxide anion radical and the other peak may be due to the reduction of the anthraquinone (A) to the corresponding semiquinone. Hydrated and/or protonated, the hydroperoxide anion radicals can release superoxide as outlined below (Eqs. (4)–(6)) [8]

$$A + e^- \rightarrow A^{\bullet -} \quad (4)$$

$$A^{\bullet -} + O_2 \rightarrow AO_2^{\bullet -} \quad (5)$$

$$AO_2^{\bullet -} \rightarrow A + O_2^{\bullet -} \quad (6)$$

Electron donating substituents cause a shift of $E_{1/2}$ to more negative value whereas electron withdrawing substituents

Table 1
Cyclic voltammetric data of HQ, AQ and QZ

| Substrate | Wave I peak potential[a] | | | | Wave II peak potential[a] | | | |
|---|---|---|---|---|---|---|---|---|
| | $E_{pc}$ | $E_{pa}$ | $\Delta E_p$ | $E_{1/2}$ | $E_{pc}$ | $E_{pa}$ | $\Delta E_p$ | $E_{1/2}$ |
| QZ | −0.670 | −0.580 | 0.090 | −0.625 | −1.12 | −1.04 | 0.08 | −1.075 |
| AQ | −0.520 | −0.450 | 0.070 | −0.485 | −0.91 | −0.83 | 0.08 | −0.870 |
| HQ | −0.692 | −0.635 | 0.057 | −0.664 | −1.06 | −1.01 | 0.05 | −1.036 |

[a] Potential in *V* against Ag/AgCl, scan rate: 100 mV/s.

cause the opposite effect [36]. HQ, which possesses the electron releasing hydroxyethyl group, shows more negative shift than AQ and QZ. Hence it may favour the enzymatic reduction by cytochrome reductase: NADH system to generate semiquinone radical that on reaction with molecular oxygen to generate superoxide [37,38]. In addition, of the three anthraquinones, the electron transfer process of HQ is highly reversible as shown by the $\Delta E_p$ value (−0.057 V). This suggests that the reductively activated intermediate of HQ is stable and can undergo redox cycling to generate $O_2^{\bullet -}$. The superoxide generation order HQ > AQ > QZ also follows the reversible nature ($\Delta E_p$ value) of the one electron reduction couple.

## 4. Conclusion

Three anthraquinone derivatives have been investigated for their ability to generate ROS by photo- as well as enzymatic reduction. RNO bleaching method, EPR spectroscopy, SOD inhibitable ferricytochrome *c* reduction assay and EPR spin trapping experiments show that both Type I and Type II mechanisms are involved in the photosensitization of anthraquinones derivatives. Higher yields of $O_2^{\bullet -}$ were observed for the quinone HQ, possessing an electron releasing substituents.

## Acknowledgements

One of us (K.K. Mothilal) thanks UGC, New Delhi for granting the Teacher Fellowship (FIP) and the management of Saraswathi Narayanan College, Madurai, India for leave. We also thank the UGC, India for the special assistance under DRS scheme.

## References

[1] J.W. Lown, Chem. Soc. Rev. (1993) 165.
[2] D.O. Anderson, N.D. Weber, S.G. Wood, B.G. Hughes, B.K. Murray, J.A. North, Antiviral Res. 16 (1991) 185.
[3] G. Powis, Pharmac. Ther. 35 (1987) 57–162.
[4] H.W. Moore, R. Czerniak, A. Hamdan, Drugs Exptl. Clin. Res. XII (6/7) (1986) 475.
[5] T. Kimachi, K. Sugita, Y. Tamura, M. Kagawa, K. Yamasaki, F. Yoneda, T. Sasaki, Bioinorg. Medi. Chem. Lett. 7 (1997) 753.
[6] D. Jeziorek, T. Ossowski, A. Liwo, D. Dyl, M. Nowacka, W. Woznicki, J. Chem. Soc., Perkin Trans. 2 (1997) 229.
[7] T. Hiwasa, Y. Arase, Z. Chen, K. Kita, K. Vme Zawa, H. Ito, N. Suzuki, FEBS Lett. 44 (1999) 173.
[8] K.J. Reszka, P. Kolodziejczyk, J.W. Lown, Free Radic. Biol. Med. 2 (1986) 267.
[9] K.J. Reszka, P. Bilski, C.F. Chignell, J.A. Hartley, N. Khan, R.L. Souhami, A.J. Mendoca, J.W. Lown, J. Photochem. Photobiol. 15 (1992) 317.
[10] J. Johnson Inbaraj, M.C. Krishna, R. Gandhidasan, R. Murugesan, Biochem. Biophys. Acta 1472 (1999) 462.
[11] D.P. Specht, P.A. Matric, S. Farid, Tetrahedron 38 (1982) 1203.
[12] K.B. Mullah, J.K. Sutherland, Tetrahedron Lett. 28 (1987) 2065.
[13] I. Kraljic, A. El Mohsni, Photochem. Photobiol. 28 (1978) 577.
[14] J. Johnson Inbaraj, R. Gandhidasan, S. Subramanian, R. Murugesan, J. Photochem. Photobiol. Chem. A 117 (1998) 21.
[15] J.M. McCord, I. Fridovich, J. Biol. Chem. 244 (1969) 6049.
[16] W.H. Koppenol, J. Butler, Isr. J. Chem. 24 (1984) 11.
[17] M.C. Krishna, S. Uppuluri, P. Riesz, J.S. Ziglet Jr., D. Balasubramanian, Photochem. Photobiol. 54 (1991) 51.
[18] A. Constantinescu, D. Han, L. Packer, Vitamin E recycling in human erythrocyte membranes, J. Biol. Chem. 268 (1993) 10906.
[19] Y. Lion, M. Delmelle, A. Van de Vorst, Nature 263 (1976) 442.
[20] E. Gandin, Y. Lion, A. Van de Vorst, Photochem. Photobiol. 37 (1983) 271.
[21] E. Wilkinson, J.G. Brummer, J. Phys. Chem. Ref. Data 10 (1981) 809.
[22] M.A.J. Rodgers, Photochem. Photobiol. 37 (1983) 99;
J.D. Balentine, Pathway of Oxygen Toxicity, Academic Press, New York, 1982.
[23] E. Ben-Hur, A. Carmichael, P. Riesz, I. Rosenthal, Int. J. Radiat. Biol. 48 (1985) 837;
E. Finkelstein, G.M. Rosen, E.J. Rauckman, Mol. Pharmac. 21 (1982) 262.
[24] J.V. Bannister, in: R.A. Greenwald (Ed.), CRC Handbook of Methods for Oxygen Radical Research, CRC Press, Boca Raton, FL, 1985, p. 153.
[25] J. Harbour, V. Chew, J.R. Bolton, Can. J. Chem. 52 (1974) 3549;
J.B. Feix, B. Kalyanaraman, Arch. Biophys. 291 (1991) 43.
[26] A.E. Alergia, A. Ferrer, E. Sepulveda, Photochem. Photobiol. 66 (1997) 436.
[27] S. Monroe, S.S. Eaton, Arch. Biochem. Biophys. 329 (1996) 221.
[28] L. Eberson, J. Chem. Soc., Perkin Trans. 2 (1994) 171.
[29] A.E. Alegria, A. Ferrer, G. Santiago, E. Sepulveda, W. Flores, J. Photochem. Photobiol. 127 (1999) 57.
[30] J.W. Lown, Anthracycline and Anthracyclinedione-based Anticancer Drugs, Elsevier, Amsterdam, 1988.
[31] J.H. Doroshow, K.J.A. Davies, J. Biol. Chem. 261 (1986) 3068.
[32] J. Tarasiuk, A. Liwo, S. Wojtkowiak, M. Dzieduszycka, A. Temppezyk, A. Gaenier Suillerot, S. Martelli, E. Borowski, Anti-cancer Drug Des. 6 (1992) 399.
[33] J.W. Lown, H.H. Chen, J.A. Plambeck, E.M. Acton, Biochem. Pharmacol. 28 (1979) 2563.
[34] H. Berg, G. Horn, W. Ihnr, J. Antibiot. 35 (1982) 800.
[35] B. Halliwell, O.I. Aruoma (Eds.), DNA and Free Radicals, Ellis Horword, New York, 1990, pp. 243–265.
[36] C. Hansch, A. Leo, S.H. Vnger, K.H. Kim, D. Nikaitaini, E.J. Lien, Anticancer Res. 6 (1986) 605.
[37] B.A.S. Vingen, G. Powis, Arch. Biochem. Biophys. 209 (1981) 119.
[38] J.W. Lown, H.H. Chen, J.A. Plambeck, Biochem. Pharmacol. 4 (1982) 575.